

## Effects of work function on thermal sensitivity of electrode potential

Hyuck Lim,<sup>1</sup> Yang Shi,<sup>1</sup> Meng Wang,<sup>2</sup> and Yu Qiao<sup>1,2,a)</sup>

<sup>1</sup>Program of Materials Science and Engineering, University of California – San Diego, La Jolla, California 92093, USA

<sup>2</sup>Department of Structural Engineering, University of California – San Diego, La Jolla, California 92093-0085, USA

(Received 21 March 2015; accepted 14 May 2015; published online 2 June 2015)

In recently developed thermally chargeable supercapacitors, temperature dependent capacitive effect is employed to harvest and store low-grade heat as electric energy, for which a key factor dominating the system performance is the thermal sensitivity of electrode potential ( $dV/dT$ ). In the current study, the influence of electrode material properties, particularly the work function, is analyzed through a set of thermal-to-electric energy conversion experiments. The testing data suggest that  $dV/dT$  increases monotonously with the work function. This finding sheds light on electrode materials selection. © 2015 AIP Publishing LLC. [<http://dx.doi.org/10.1063/1.4921769>]

To enhance energy security and to reduce energy-related greenhouse gas emissions, it is critical to better utilize the energy that is currently being wasted and/or regarded harmful. One of the important energy sources is low-grade heat (LGH), thermal energy with the temperature ( $T$ ) lower than  $300^{\circ}\text{C}$ – $400^{\circ}\text{C}$ ,<sup>1</sup> such as the waste heat in coal and nuclear power plants, solar thermal energy, and geo-thermal energy. If LGH can be harvested with a high efficiency, from coal power plants alone, many Giga-Watt of additional power can be generated in U.S.<sup>2</sup> For another example, today's best solar panels can convert only  $\sim 16\%$  of solar energy to electricity;<sup>3</sup> the rest of energy is eventually dissipated as LGH. The Carnot cycle limit for un-concentrated solar thermal energy is  $\sim 10\%$ . If the waste LGH can be harvested with an efficiency of  $5\%$ – $8\%$ , the overall solar to electrical energy conversion efficiency of solar panel can be increased by nearly  $50\%$ .

However, the relatively low temperature associated with LGH demands a high system efficiency, which cannot be achieved by conventional thermal-to-electric energy conversion (TEEC) technologies, including the direct TEEC techniques based on the Seebeck effect and the indirect TEEC techniques such as organic Rankin cycle (ORC) machines.<sup>4</sup> The major issue of the indirect methods is the high cost, typically more than a few dollars per Watt,<sup>5</sup> due to the high installation, maintenance, and operational costs. The main technical difficulty of thermoelectric materials is thermal shorting, i.e., as electrons move from the high-temperature side to the low-temperature side, heat conduction also occurs.<sup>6</sup>

Searching for better TEEC techniques for LGH has been an active area of study for the past decade.<sup>7</sup> A TEEC process must be based on one or multiple physical and/or chemical phenomena that are both thermally and electrically sensitive. Recently, in a research on thermally induced capacitive effect,<sup>8–13</sup> we developed thermally chargeable supercapacitors (TCS). In a TCS, two half-supercapacitors are placed at different temperatures, as depicted in Fig. 1. Each half-supercapacitor consists of

an electrode immersed in an electrolyte solution. At the solid-liquid interface, the solvated ions are subjected to anisotropic force fields and form a double layer. Thus, a certain amount of electric energy is stored as surface charges. A potential difference is generated between the electrode and the liquid phase, which is referred to as electrode potential. As temperature varies, accompanied by the change in effective surface ion density, the electrode potential becomes different. Consequently, when the two electrodes are connected, a net output voltage can be measured. If the electrode is a nanoporous material of an ultrahigh surface area ( $10^2$ – $10^3$   $\text{m}^2/\text{g}$ ), the capacitance can be quite high, leading to a high energy density. The TCS works in the LGH temperature range, below  $100^{\circ}\text{C}$  if the liquid phase is aqueous. Due to the high mobility of the surface ions, even with a small temperature difference of only a few tens of  $^{\circ}\text{C}$ , the output voltage ( $V$ ) can be on the scale of  $10^2$  mV, higher than that of thermoelectric materials by more than an order of magnitude. With a constant internal impedance, the harvested and stored electric energy by a TCS are proportional to  $V^2$ . It is

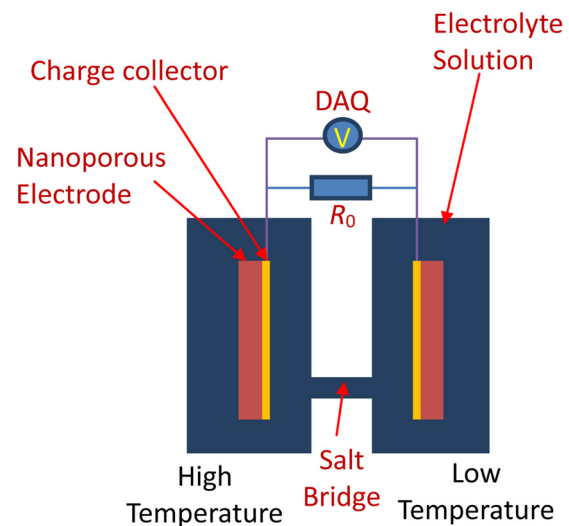


FIG. 1. Schematic of a TCS, formed by two identical electrodes separately immersed in an electrolyte solution.

<sup>a)</sup>Author to whom correspondence should be addressed. Electronic mail: yqiao@ucsd.edu. Tel.: +1-858-534-3388.

clear that, in order to enhance the TCS performance, the thermal sensitivity of electrode potential,  $dV/dT$ , must be as high as possible.

The experimental setup is shown in Fig. 1. Two identical electrodes were immersed in 21 wt. % formamide (FA) solution of lithium chloride (LiCl). The electrodes were made of foils of platinum (Pt), nickel (Ni), copper (Cu), or indium (In). The rationale of choosing these materials will be discussed below. The two electrodes were placed in two 50 ml containers, separately. The containers were connected by a salt bridge, with the diameter of  $\sim 5$  mm and the length of  $\sim 30$  mm. By using a cold water bath, one of the containers was kept at room temperature ( $T_r$ ). The other container was heated by a Corning PC220 heat plate, with the heating rate of  $\sim 3^\circ\text{C}/\text{min}$ . The temperatures of the two electrodes were monitored by type-K thermocouples connected to a National Instrument HH-20A Reader.

As the temperature difference between the two electrodes ( $\Delta T$ ) increased, a significant output voltage,  $V$ , was measured between the two electrodes by a National Instrument SCB68 data acquisition (DAQ) system. Figure 2 shows typical  $V$ - $\Delta T$  curves for the four materials under investigation, based on which the average thermal sensitivity of electrode potential,  $dV/dT$ , was calculated, as shown in Fig. 3. For self-comparison purpose and for the sake of simplicity, the average  $dV/dT$  was taken as  $V_{\text{max}}/\Delta T_{\text{max}}$ , where  $V_{\text{max}}$  and  $\Delta T_{\text{max}}$  are the maximum potential difference and the maximum temperature difference, respectively. It qualitatively describes how rapidly the output voltage increases with temperature.

The electrode materials are so-chosen in order to test our hypothesis that the thermal sensitivity of electrode potential is related to the work function (WF). Work function is a concept in solid state physics, defined as the minimum energy that is required to remove an electron from the Fermi level to vacuum.<sup>14</sup> For the metallic materials investigated in the current study, the conduction band is partly filled and the Fermi level is inside the band.<sup>15</sup> The value of WF is typically a few eV, depending on a number of factors such as the packing mode of atoms and the crystallographic orientation. Work function is closely correlated to the

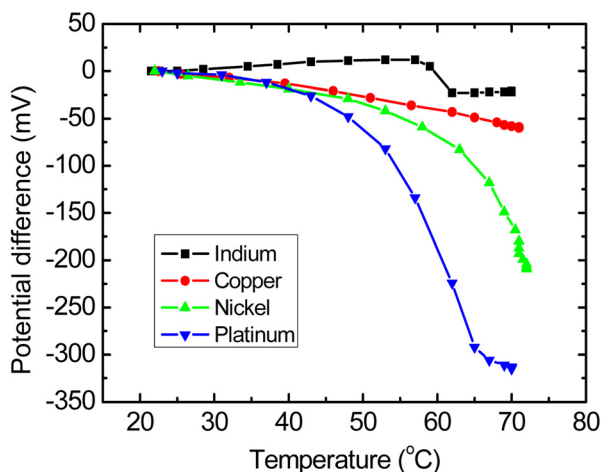


FIG. 2. Typical results of the output voltage ( $V$ ) as a function of the temperature difference ( $\Delta T$ ).

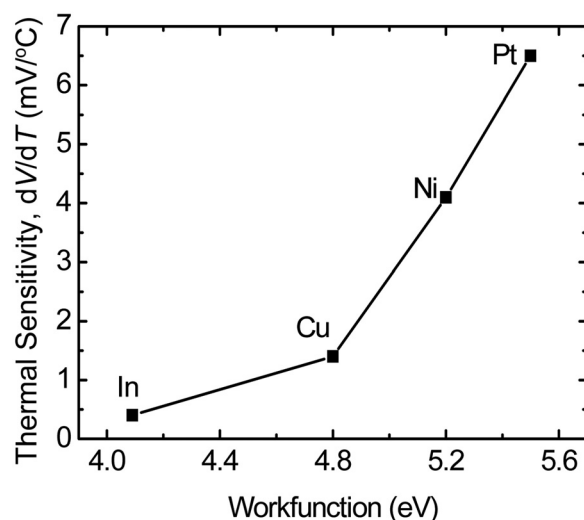


FIG. 3. The relationship between the thermal sensitivity of electrode potential ( $dV/dT$ ) and the work function.

ionization energy and insensitive to the surface charges. It can be calculated as  $WF = W_d - E_F$ , where  $W_d$  is the potential difference caused by surface dipole and  $E_F$  is the Fermi energy. According to the literature data,<sup>15</sup> the values of WF of In, Cu, Ni, and Pt are 4.1 eV, 4.8 eV, 5.2 eV, and 5.5 eV, respectively.

In the classic Gouy-Chapman model,<sup>16</sup> the adsorbed ion structure at a solid-liquid interface is simplified as an electric double layer, consisting of two capacitive components: One from the Helmholtz layer,  $C_H$ , and the other from the diffusion layer,  $C_D$ , as depicted in Fig. 4. While this model is useful to explain many surface phenomena, e.g., the temperature dependence of electrode potential and surface tension, it does not directly capture the influence of the solid phase. According to the Jellium model,<sup>17</sup> a third capacitive component,  $C_M$ , may be taken into consideration. It comes from the electron spillover over the electrode surface and can result in an asymmetric electron distribution, leading to the formation of a relatively strong dipole moment. Due to the shielding effect,<sup>16</sup> when the electrode phase varies, the major changes take place in the  $C_M$  layer, and the variations in  $C_H$  and  $C_D$  are secondary.

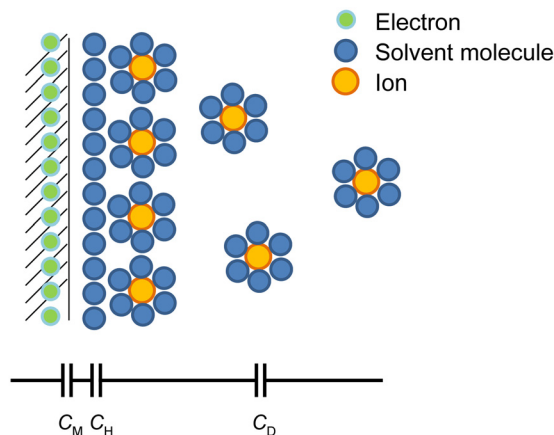


FIG. 4. Schematic of surface ion structure.

The change in potential difference between the bulk liquid phase and the electrode surface ( ${}^M\Delta^S\phi$ ) is over all the three capacitive components;<sup>17</sup> that is,

$${}^M\Delta^S\phi = \frac{Q}{C_{\text{total}}} = \frac{Q}{C_M} + \frac{Q}{C_H} + \frac{Q}{C_D}, \quad (1)$$

where  $Q$  is the effective surface charge and  $C_{\text{total}}$  is the effective capacitance of the double layer structure caused by the three capacitive components. The distribution of the surface charge is determined by the temperature and the electric field within the diffusion layer, which can be described by the Poisson-Boltzman equation.<sup>18</sup> If the temperature in the double layer changes, the effective density of the ionic charges in the diffusion layer should vary accordingly, by an amount of  $\Delta Q$ . At the equilibrium condition, the changes in effective charges in all the capacitive components are the same. The contribution of the electrode phase to the temperature induced change in potential difference can be written as

$$\frac{d({}^M\Delta^S\phi)_M}{dT} = \frac{d}{dT} \left( \frac{Q}{C_M} \right) = \frac{1}{C_M} \left\{ \frac{dQ}{dT} - ({}^M\Delta^S\phi)_M \frac{dC_M}{dT} \right\}, \quad (2)$$

where the subscript “M” indicates the contribution from the  $C_M$  layer. From Eq. (2), it can be seen that the derivative of the potential difference with respect to temperature change is proportional to  $1/C_M$ . The Jellium model describes the contribution of the electrode phase to the overall capacitance of the double layer,<sup>17</sup> in which  $C_M$  is highly dependent on the density of positive ions in the electrode ( $n_+$ )

$$\frac{1}{C_M} = -\frac{8\pi n_+ e_0}{\alpha^3} \frac{\partial \alpha}{\partial q}, \quad (3)$$

where  $\alpha$ ,  $e_0$ , and  $q$  are semi-empirical parameters capturing the effects of the electronic density profile, the electronic charge, and the surface charge density, respectively. From Eqs. (2) and (3), it can be derived that the partial potential change is proportional to the density of positive ions ( $n_+$ ), which is correlated to the work function: A metallic material that has a high  $n_+$  value usually also has a large WF.

The four electrode materials under investigation have quite different work functions,<sup>15</sup> among which In has the lowest WF. According to Fig. 2, when temperature changes by nearly 50 °C, the measured electrode potential of In is quite random, probably reflecting the drifting of the internal grounding. The average temperature sensitivity ( $dV/dT$ ) is only 0.4 mV/K, as shown in Fig. 3. When the electrode material is changed to Cu, the WF value increases to 4.8 eV, and it is evident that the electrode potential increases with the temperature. The average temperature sensitivity is 1.4 mV/K. For Ni and Pt, the WF values are even much higher, and  $dV/dT$  are 4.1 mV/K and 6.5 mV/K, respectively, both higher than that of Cu. It is clear that  $dV/dT$  is positively correlated to WF, fitting well with the prediction of the Jellium model.

Note that except for In, for which the voltage change is quite small and the measurement results are governed by data scatter, for the rest of the three electrode materials (Cu, Ni, and Pt)  $dV/dT$  is relatively linear to WF

(Fig. 3), suggesting that the first order approximation used in the above analysis is plausible.

Note that our definition of  $dV/dT$  does not capture the nonlinearity in the  $V-\Delta T$  relationship. Figure 2 shows that the temperature dependence of electrode potential is quite nonlinear. For Cu, Ni, and Pt, the increase in electrode potential is relatively slow when the temperature is low, and  $V$  rises increasingly fast with temperature. The change in electrode potential is related to the variation in the effective adsorption coverage, which can be promoted as  $T$  is higher.<sup>9</sup>

In summary, as temperature changes, due to the associated charge motion, the potential difference across the double layer of an electrode-electrolyte interface would vary. The temperature sensitivity of electrode potential is higher if the electrode material has a higher work function. This effect may be explained by the Jellium model, having important relevance to the optimization of the electrode materials in thermally chargeable supercapacitors for harvesting and storing low-grade heat.

The concept development was supported by the State of California EISG Program under Grant No. EISG-08-13. The concept validation was supported by the National Science Foundation under Grant No. IIP-1045681. The experimental system development was supported by the National Science Foundation under Grant No. ECCS-1028010. The data analysis was supported by the Advanced Research Projects Agency – Energy under Grant No. DE-AR0000396.

<sup>1</sup>B. F. Tchanche, G. Lambrinos, A. Frangoudakis, and G. Papadakis, *Renewable Sustainable Energy Rev.* **15**, 3963 (2011).

<sup>2</sup>F. Velez, J. J. Segovia, M. Carmen Martin, G. Antolin, F. Chejne, and A. Quiiano, *Renewable Sustainable Energy Rev.* **16**, 4175 (2012).

<sup>3</sup>K. Mertens, *Photovoltaics: Fundamentals, Technology and Practice* (Wiley, 2014).

<sup>4</sup>J. Bao and L. Zhao, *Renewable Sustainable Energy Rev.* **24**, 325 (2013).

<sup>5</sup>C. Sprouse III and C. Depcik, *Appl. Therm. Eng.* **51**, 711 (2013).

<sup>6</sup>M. H. Elsheikh, D. A. Shnawah, M. F. M. Sabri, S. B. M. Said, M. H. Hassan, M. B. A. Bashir, and M. Mohamad, *Renewable Sustainable Energy Rev.* **30**, 337 (2014).

<sup>7</sup>A. W. Crook, “Profiting from low-grade heat,” *The Watt Committee on Energy Report No. 26* (Institution of Engineering and Technology, 1994).

<sup>8</sup>H. Lim, C. Zhao, and Y. Qiao, “Performance of thermally chargeable supercapacitors in different solvents,” *Phys. Chem. Chem. Phys.* **16**, 12728–12730 (2014).

<sup>9</sup>H. Lim, W. Lu, X. Chen, and Y. Qiao, “Effects of ion concentration on thermally chargeable double-layer supercapacitors,” *Nanotechnology* **24**, 465401 (2013).

<sup>10</sup>H. Lim, W. Lu, and Y. Qiao, “Dependence on cation size of thermally induced capacitive effect of a nanoporous carbon,” *Appl. Phys. Lett.* **101**, 063902 (2012).

<sup>11</sup>H. Lim, W. Lu, X. Chen, and Y. Qiao, “Anion size effect on electrode potential in a nanoporous carbon,” *Int. J. Electrochem. Sci.* **7**, 2577–2583 (2012).

<sup>12</sup>Y. Qiao, V. K. Punyamurtula, A. Han, and H. Lim, “Thermal-to-electric energy conversion of a nanoporous carbon,” *J. Power Sources* **183**, 403–405 (2008).

<sup>13</sup>T. Kim, W. Lu, H. Lim, A. Han, and Y. Qiao, “Electrically controlled hydrophobicity in a surface modified nanoporous carbon,” *Appl. Phys. Lett.* **98**, 053106 (2011).

<sup>14</sup>J. W. Mayer and S. S. Lau, *Electronic Materials Science* (Maxwell Macmillan, 1990), Chap. 4.

<sup>15</sup>L. F. Deis, *CRC Handbook of Chemistry and Physics* (CRC, 2009).

<sup>16</sup>J. O. M. Bockris, A. K. N. Reddy, and M. Gamboa-Aldeco, *Modern Electrochemistry* (Plenum Press, 1970), Vol. 2A.

<sup>17</sup>J. Goodisman, *Electrochemistry: Theoretical Foundations* (Wiley, 1987).

<sup>18</sup>J. O’M. Bockris, Amulya K. N. Reddy, and M. Gamboa-Aldeco, *Modern Electrochemistry*, 2nd ed. (Springer, 1973), Vol. 2A, Chap. 6, p. 1000.